
Symmetry Teleportation for Accelerated Optimization

Bo Zhao

University of California, San Diego
bozhao@ucsd.edu

Nima Dehmamy

IBM Research
nima.dehmamy@ibm.com

Robin Walters

Northeastern University
r.walters@northeastern.edu

Rose Yu

University of California, San Diego
roseyu@ucsd.edu

Abstract

Existing gradient-based optimization methods update parameters locally, in a direction that minimizes the loss function. We study a different approach, symmetry teleportation, that allows parameters to travel a large distance on the loss level set, in order to improve the convergence speed in subsequent steps. Teleportation exploits symmetries in the loss landscape of optimization problems. We derive loss-invariant group actions for test functions in optimization and multi-layer neural networks, and prove a necessary condition for teleportation to improve convergence rate. We also show that our algorithm is closely related to second order methods. Experimentally, we show that teleportation improves the convergence speed of gradient descent and AdaGrad for several optimization problems including test functions, multi-layer regressions, and MNIST classification. Our code is available at <https://github.com/Rose-STL-Lab/Symmetry-Teleportation>.

1 Introduction

Consider the optimization problem of finding $\operatorname{argmin}_w \mathcal{L}(w)$, where \mathcal{L} is a loss function and w are the parameters. While finding global minima of $\mathcal{L}(w)$ is hard for non-convex problems, we can use gradient descent (GD) to find local minima. In GD we apply the following update rule at every step:

$$w_{t+1} \leftarrow w_t - \eta \nabla \mathcal{L}, \quad (1)$$

where η is the learning rate. Gradient descent is a first-order method that uses only gradient information. It is easy to compute but suffers from slow convergence. Second-order methods such as Newton's method use the second derivative to account for the landscape geometry. These methods enjoy faster convergence, but calculating the second derivative (Hessian) can be computationally expensive over high dimensional spaces (Hazan, 2019).

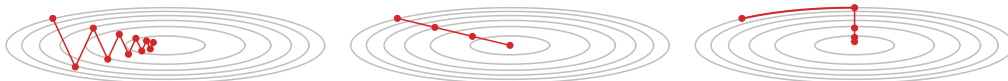


Figure 1: Left to right: gradient descent, second-order methods, proposed method.

In this paper, we propose a new optimization method based on parameter space symmetries, which are group actions on the parameter space that leave the loss unchanged. Our algorithm takes advantage

of higher-order landscape geometry but uses only gradient information in most steps, thus avoiding the computational cost of second-order methods.

Specifically, we look beyond local optimization and ask: *what if we allow the parameters to make a big jump once in a while?* As shown in Figure 1, during optimization, we teleport the parameters to another point with steeper gradients using a loss-invariant symmetry transformation. After teleportation, the loss stays the same, but the gradient and hence the rate of loss decay changes. The increased magnitude of the gradient can reduce the number of steps required to converge, leading to acceleration of the gradient descent.

The locality of gradient descent is reflected in its formulation in terms of a proximal term; our method circumvents this locality by teleporting to new locations with the same loss. A step of GD is equivalent to the following proximal mapping (Combettes and Pesquet, 2011). Let $\langle \cdot, \cdot \rangle$ denote the inner product, we have

$$\mathbf{w}_{t+1} = \operatorname{argmin}_{\mathbf{w}} \left\{ \eta \langle (\nabla \mathcal{L})|_{\mathbf{w}_t}, \mathbf{w} \rangle + \frac{1}{2} \|\mathbf{w} - \mathbf{w}_t\|_2^2 \right\}. \quad (2)$$

The term $\frac{1}{2} \|\mathbf{w} - \mathbf{w}_t\|_2^2$ is the proximal term that keeps \mathbf{w}_{t+1} close to \mathbf{w}_t . Adaptive gradient methods define the proximal term using the Mahalanobis distance $\|\mathbf{w} - \mathbf{w}_t\|_{G^{-1/2}}^2$ to account for landscape geometry. For example, in AdaGrad, G is the sum of the outer product of gradients (Duchi et al., 2011). Our proposed teleportation technique relaxes the requirement from the proximal term. We teleport to points on the same level set of $\mathcal{L}(\mathbf{w}_t)$, but allow \mathbf{w} to be far from \mathbf{w}_t in Euclidean distance.

In summary, our main contributions are:

- We propose *symmetry teleportation*, an accelerated gradient-based optimization algorithm that exploits symmetries in the loss landscape.
- We derive loss-invariant group actions of test functions and multi-layer neural networks.
- We provide necessary conditions and examples of when teleportation improves convergence rate of the current and subsequent steps.
- We show that our algorithm is closely related to second-order methods.
- Experimentally, we show that teleportation improves the convergence speed of gradient descent and AdaGrad in various optimization problems.

2 Related Work

Continuous parameter space symmetries have been identified in neural networks with homogeneous (Badrinarayanan et al., 2015; Du et al., 2018) and radial activation functions (Ganev et al., 2021). The effect of symmetry transformations on gradients has been examined for translation, scale, and rescale symmetries in Kunin et al. (2021). We contribute to this line of work by deriving loss-invariant group actions in multi-layer neural networks with invertible activation functions.

Several works exploit symmetry to facilitate optimization. For example, Path-SGD (Neyshabur et al., 2015) improves optimization in ReLU networks by path regularization. \mathcal{G} -SGD (Meng et al., 2019) performs weight updates in a scale-invariant space, which also exploits the symmetry in ReLU networks. Van Laarhoven (2017) analyzes the effect of L2 regularization in batch normalization which gives scale-invariant functions. Bamler and Mandt (2018) transforms parameters in the symmetry orbits to address slow movement along directions of weakly broken symmetry and find the optimal $g \in G$ that minimizes $\mathcal{L}(g \cdot \mathbf{w})$. In comparison, we search within G -orbits for points which maximize $|d\mathcal{L}(g \cdot \mathbf{w})/dt| = \|\nabla \mathcal{L}(g \cdot \mathbf{w})\|^2$.

Natural gradient (Amari, 1998), adaptive gradient methods (Duchi et al., 2011; Kingma and Ba, 2015), and their approximations (Martens and Grosse, 2018; Gupta et al., 2018) improve the direction of parameter updates instead of directly transforming parameters. If the group acts transitively on the level set, and we teleport to the point with maximum gradient, then our update direction is the same as that in Newton’s method. We prove that our algorithm is connected to second-order optimization methods and show that teleportation can be used to improve these methods empirically.

The concept of neural teleportation was first explored using quiver representation theory (Armenta and Jodoin, 2021; Armenta et al., 2020). These works provide a way to explore level curves of the loss

of neural networks and show that random teleportation speeds up gradient descent experimentally and theoretically. Our algorithm improves neural teleportation by searching for teleportation destinations that lead to the largest improvement in the magnitude of gradient.

Several works study how parameter initialization affects convergence rate (Saxe et al., 2014; Tarmoun et al., 2021; Min et al., 2021). If we apply a group transformation only at initialization, our method is similar to that of Tarmoun et al. (2021). We do not guarantee that the transformed parameters lead to faster convergence rate throughout the entire training. However, we accelerate convergence at least for a short time after initialization. Additionally, our method is not restricted to initialization and can be applied at any time during training.

Most contemporary neural networks are overparametrized. While this has been shown to improve generalization (Belkin et al., 2019), an important question is how overparametrization affects optimization. A series of works starting from Arora et al. (2018) show that overparametrization resulting from the depth of a neural network accelerates convergence. Another view is that the symmetry created by overparametrization poses constraints on trajectories in the form of conserved quantities (Gluch and Urbanke, 2021). Additionally, the symmetry generates additional trajectories. When the trajectories created by overparametrization are equivalent, model compression by removing symmetry reduces training time (Ganev et al., 2021). However, when trajectories are not equivalent, gradient flows on some paths are faster than others. We search for the better paths created by overparametrization.

3 Symmetry Teleportation

We propose *symmetry teleportation*, an accelerated gradient-based optimization algorithm that exploits symmetries in the loss landscape. Symmetry teleportation searches for the best gradient descent trajectory by teleporting parameters to a point with larger gradients using a group action. The resulting algorithm requires only gradient computations but is able to account for the global landscape geometry, leading to faster loss decay.

Let the group G be a set of symmetries which leave the loss function \mathcal{L} invariant: $\mathcal{L}(g \cdot (\mathbf{w}, X)) = \mathcal{L}(\mathbf{w}, X)$, where $g \in G$. We perform gradient descent for t_{max} steps. We define an index set $K \subseteq \{0, 1, 2, \dots, t_{max} - 1\}$ as a teleportation schedule. At epochs that are in the schedule, we transform parameters using group element $g \in G$ to the location where the gradient is largest, then continue with gradient descent. Algorithm 1 describes the details of this procedure. Note that the loss does not change after teleportation (Line 2-5) since \mathcal{L} is G -invariant.

Algorithm 1: Symmetry Teleportation

Input: Loss function $\mathcal{L}(\mathbf{w})$, learning rate η , number of epochs t_{max} , initialized parameters \mathbf{w}_0 , symmetry group G , teleportation schedule K .

Output: $\mathbf{w}_{t_{max}}$.

```

1 for  $t \leftarrow 0$  to  $t_{max} - 1$  do
2   if  $t \in K$  then
3      $g \leftarrow \operatorname{argmax}_{g \in G} \|(\nabla \mathcal{L})|_{g \cdot \mathbf{w}_t}\|^2$ 
4      $\mathbf{w}_t \leftarrow g \cdot \mathbf{w}_t$ 
5   end if
6    $\mathbf{w}_{t+1} \leftarrow \mathbf{w}_t - \eta(\nabla \mathcal{L})|_{\mathbf{w}_t}$ 
7 end for
8 return  $\mathbf{w}_{t_{max}}$ 

```

Algorithm 1 can be generalized to apply teleportation to stochastic gradient descent (Appendix A.1). We discuss some design choices below and provide detailed analysis in the next two sections.

When the action of G is continuous, teleportation can be implemented by parameterizing and performing gradient ascent on g . For example, the $SO(2)$ group can be parameterized by the rotation angle θ . Small transformations $g \in GL_d(\mathbb{R})$ (general linear group) can be parameterized as $g \approx I + \varepsilon T$ where $\varepsilon \ll 1$ and T are arbitrary $d \times d$ matrices. For discrete groups, search algorithms or random sampling can be used to find a group element that improves the magnitude of the gradient.

Although $g \cdot (\mathbf{w}, X)$ does not change X in the cases we consider in this paper, Algorithm 1 can be extended to allow transformations on both parameters and data. The group actions on data during

teleportations can be precomposed and applied to the input data at inference time. The algorithm extension that allows transformation on the input can be found in Appendix A.2.

The teleportation schedule K is a hyperparameter that determines when to perform teleportation. We define K as a set to allow flexible teleportation schedules, such as with non-fixed frequencies or teleporting only at the earlier epochs.

4 Symmetry Groups of Certain Optimization Problems

We give a few practical examples to demonstrate how teleportation can be used to accelerate optimization. Specifically, we first consider two test functions which are often used to evaluate optimization algorithms (Back, 1996). We then derive the symmetries of multi-layer neural networks.

4.1 Test functions

Rosenbrock function. The Rosenbrock function originally introduced by Rosenbrock (1960) has a characteristic global minimum that is inside a long, narrow, parabolicly-shaped flat valley. Finding the valley is easy but reaching the minimum is difficult. On a 2-dimensional space, the Rosenbrock function has the following form:

$$\mathcal{L}_r(x_1, x_2) = 100(x_1^2 - x_2)^2 + (x_1 - 1)^2. \quad (3)$$

Booth function. The Booth function (Jamil and Yang, 2013) is also defined on \mathbb{R}^2 and has one global minimum at $(1, 3)$ where the function evaluates to 0:

$$\mathcal{L}_b(x_1, x_2) = (x_1 + 2x_2 - 7)^2 + (2x_1 + x_2 - 5)^2. \quad (4)$$

The following proposition identifies the symmetry of these two test functions.

Proposition 4.1. *The Rosenbrock and Booth functions have rotational symmetry. In other words, there exist action maps $a_r, a_b : \text{SO}(2) \times \mathbb{R}^2 \rightarrow \mathbb{R}^2$, such that for all $g \in \text{SO}(2)$,*

$$\mathcal{L}_r(x_1, x_2) = \mathcal{L}_r(a_r(g, [x_1, x_2])) \quad \text{and} \quad \mathcal{L}_b(x_1, x_2) = \mathcal{L}_b(a_b(g, [x_1, x_2])).$$

The exact forms of the action maps are deferred to Appendix B.1.2 and B.1.3. During the teleportation step, our goal is to maximize the gradient within a level set of the loss: $\max_{g \in \text{SO}(2)} \left\| \frac{d\mathcal{L}(g \cdot (x_1, x_2))}{dt} \right\|$.

4.2 Multi-layer Neural Networks

Next, we consider feed-forward neural networks. Denote the output of the m th layer by $h_m \in \mathbb{R}^{d_m \times n}$, where d_m is the hidden dimension and n is the number of samples. Denote the input by $h_0 = X \in \mathbb{R}^{d_0 \times n}$. In terms of the previous layer output $\tilde{h}_m = W_m h_{m-1}$ where $W_m \in \mathbb{R}^{d_m \times d_{m-1}}$ (we absorb biases into W_m by adding an extra row of ones in \tilde{h}_{m-1}), the output h_m is

$$h_m = \sigma(\tilde{h}_m) = \sigma(W_m h_{m-1}). \quad (5)$$

We assume the activation functions $\sigma : \mathbb{R} \rightarrow \mathbb{R}$ are bijections. For instance, Leaky-ReLU is bijective. For other activation, such Sigmoid or Tanh, we analytically extend them to bijective functions (e.g. $\tanh(x) + e^{x-N} - e^{-x+N}$ for $N \gg 1$). For linear activations, we have linear symmetries:

Proposition 4.2. *A linear network is invariant under all groups $G_m \equiv \text{GL}_{d_m}$ acting as*

$$g \cdot (W_m, W_{m-1}) = (W_m g^{-1}, g W_{m-1}), \quad g \cdot W_k = W_k, \quad \forall k \notin \{m, m-1\}. \quad (6)$$

Similar, in the nonlinear case, we want to find $g \cdot W_m$ that keep the outputs h_k for $k \neq m-1$ invariant. With nonlinearity, $\tilde{h}_m = W_m \sigma(W_{m-1} h_{m-2})$. This network has a $\text{GL}_{d_{m-1}}$ symmetry given by

$$g \cdot (W_m, h_{m-1}) = (W_m g^{-1}, g h_{m-1}), \quad g \cdot h_m = W_m g^{-1} g h_{m-1} = h_m. \quad (7)$$

Thus, we have the following proposition regarding symmetries of nonlinear networks:

Proposition 4.3. Assume that h_{m-2} is invertible. A multi-layer network with bijective activation σ has a $\text{GL}_{d_{m-1}}$ symmetry. For $g_m \in G_m = \text{GL}_{d_{m-1}}(\mathbb{R})$ the following group action keeps h_p with $p \geq m$ invariant

$$g_m \cdot W_k = \begin{cases} W_m g_m^{-1} & k = m \\ \sigma^{-1}(g_m \sigma(W_{m-1} h_{m-2})) h_{m-2}^{-1} & k = m - 1 \\ W_k & k \notin \{m, m - 1\} \end{cases} \quad (8)$$

Proofs can be found in Appendix B.2. Note that this group action depends on the input to the network as well as the current weights of all the lower layers. Yet, since the action keeps the output of upper and lower layers invariant, multiple G_m for different m applied at the same time still keep the network output invariant. The proposition assumes that h_{m-2} is square and full-rank. When $n < d_{m-2}$ and h_{m-2} has rank n , (8) (with left inverse of h_{m-2}) keeps the loss invariant but does not satisfy the identity axiom of a group action.

5 Theoretical Analysis

5.1 What symmetries help accelerate optimization

We now discuss the conditions that need to be satisfied for teleportation to accelerate GD. For brevity, we denote all trainable parameters (e.g. $\{W_1, \dots, W_p\}$ for the p -layer neural network) by a single flattened vector $\mathbf{w} \in \mathbb{R}^n$. Consider a symmetry G of the loss function $\mathcal{L}(\mathbf{w})$, meaning for all $g \in G$, $\mathcal{L}(\mathbf{w}) = \mathcal{L}(g \cdot \mathbf{w})$. We quantify how teleportation by G changes the rate of loss decay, given by

$$\frac{d\mathcal{L}(\mathbf{w})}{dt} = \left\langle \frac{\partial \mathcal{L}}{\partial \mathbf{w}}, \frac{d\mathbf{w}}{dt} \right\rangle = -[\nabla \mathcal{L}]^T \eta \nabla \mathcal{L} = -\|\nabla \mathcal{L}\|_\eta^2, \quad (9)$$

where η is the matrix of learning rates (which must be positive semi-definite) and $\|v\|_\eta^2 = v^T \eta v$ is the Mahalanobis norm. A constant learning rate means $\eta = I$.

The following proposition provides the condition a symmetry needs to satisfy to accelerate optimization. (Proofs can be found in Appendix C.1.)

Proposition 5.1. Let $\mathbf{w}' = g \cdot \mathbf{w}$ be a point we teleport to. Let $J = \partial \mathbf{w}' / \partial \mathbf{w}$ be the Jacobian. Symmetry teleportation using g accelerates the rate of decay in \mathcal{L} if it satisfies

$$\left\| [J^{-1}]^T \nabla \mathcal{L}(\mathbf{w}) \right\|_\eta^2 > \|\nabla \mathcal{L}(\mathbf{w})\|_\eta^2. \quad (10)$$

If the action of the symmetry group $G \subset \text{GL}_n$ is linear we have $\mathbf{w}' = g \cdot \mathbf{w} = g\mathbf{w}$ and $J = g$. It follows that if G is a subgroup of the orthogonal group, $d\mathcal{L}/dt$ will be invariant:

Corollary 5.2. Let O_η denote the orthogonal group of invariances of the inverse of the learning rate, η^{-1} , meaning for $g \in O_\eta$, $g^T \eta^{-1} g = \eta^{-1}$. Then

$$\forall g \in O_\eta, \quad \frac{d\mathcal{L}(g \cdot \mathbf{w})}{dt} = \frac{d\mathcal{L}(\mathbf{w})}{dt}. \quad (11)$$

In the simple case where the learning rate is a constant, $O_\eta = O(n)$ becomes the classic orthogonal group (e.g. rotations) with $g^T g = I$. In general, when g preserves the norm of the gradient, symmetry teleportation has no effect on the convergence rate.

From Theorem 3.2 in Hazan (2019), assuming that \mathcal{L} is β -smooth and is bounded by $|\mathcal{L}| \leq M$, the gradient norm in gradient descent converges as $\frac{1}{2\beta} \sum_{t=1}^T \|(\nabla \mathcal{L})|_{\mathbf{w}_t}\| \leq 2M$. Teleportation increases $(\nabla \mathcal{L})|_{\mathbf{w}_t}$, therefore requiring less time to reach convergence.

5.2 Improvement of subsequent steps

Since teleportation moves the parameters to a point with a larger gradient, and subsequent GD steps are local, we would expect that teleportation improves the magnitude of the gradient for a few future steps as well. The following results formalize this intuition (proofs in Appendix C.2.).

Assumption 5.3 (Lipschitz Continuity). *The l2 norm of the gradient is Lipschitz continuous with constant $L \in \mathbb{R}^{\geq 0}$, which is*

$$\left\| \left\| \frac{\partial \mathcal{L}}{\partial \mathbf{w}_1} \right\|_2 - \left\| \frac{\partial \mathcal{L}}{\partial \mathbf{w}_2} \right\|_2 \right\| \leq L \|\mathbf{w}_1 - \mathbf{w}_2\|_2, \quad (12)$$

where $\mathbf{w}_1, \mathbf{w}_2$ are two points in the parameter space and L is the Lipschitz constant.

Proposition 5.4. *Consider the gradient descent with a G -invariant loss $\mathcal{L}(\mathbf{w})$ and learning rate $\eta \in \mathbb{R}^+$. Let \mathbf{w}_t be the parameter at time t and $\mathbf{w}'_t = g \cdot \mathbf{w}_t$ the parameter teleported by $g \in G$. Let \mathbf{w}_{t+T} and \mathbf{w}'_{t+T} be the parameters after T more steps of gradient descent from \mathbf{w}_t and \mathbf{w}'_t respectively. Under Assumption 5.3, if $\eta L < 1$, and*

$$\frac{\|\partial \mathcal{L} / \partial \mathbf{w}'_t\|_2}{\|\partial \mathcal{L} / \partial \mathbf{w}_t\|_2} \geq \frac{(1 + \eta L)^T}{(1 - \eta L)^T}, \quad (13)$$

then

$$\left\| \frac{\partial \mathcal{L}}{\partial \mathbf{w}'_{t+T}} \right\|_2 \geq \left\| \frac{\partial \mathcal{L}}{\partial \mathbf{w}_{t+T}} \right\|_2. \quad (14)$$

The proposition provides a sufficient condition for teleportation to improve T future steps. The condition is met when L is small, η is small, or the initial improvement, $\left\| \frac{\partial \mathcal{L}}{\partial \mathbf{w}'_t} \right\|_2 / \left\| \frac{\partial \mathcal{L}}{\partial \mathbf{w}_t} \right\|_2$, is large.

5.3 Convergence analysis for convex quadratic functions

Teleportation improves the magnitude of gradient for the current step. We have also shown that the magnitude of gradient stays large for a few subsequent steps (Proposition 5.4). In this section, we analyze a class of functions where teleporting once guarantees optimality at all future times. We consider a trajectory optimal if for every point on the trajectory, the magnitude of gradient is at a local maximum in the loss level set that contains the point.

Consider a positive definite quadratic form $\mathcal{L}_A(\mathbf{w}) = \mathbf{w}^T A \mathbf{w}$, where $\mathbf{w} \in \mathbb{R}^n$ is the parameter and $A \in \mathbb{R}^{n \times n}$ is a positive definite matrix. The gradient of \mathcal{L}_A is $\nabla \mathcal{L}_A = 2A\mathbf{w}$, and the Hessian of \mathcal{L}_A is $H = 2A$. Since A is defined to be positive definite, \mathcal{L}_A is convex. The function \mathcal{L}_A has global minimum at a single point $\mathbf{w}^* = 0$.

Let ρ be a representation of $O(n)$ acting on \mathbb{R}^n . For $g \in O(n)$, we define the following group action:

$$g \cdot \mathbf{w} = A^{-\frac{1}{2}} \rho(g) A^{\frac{1}{2}} \mathbf{w}. \quad (15)$$

Then it can be shown that $\mathcal{L}_A(\mathbf{w})$ admits a $O(n)$ symmetry:

$$\mathcal{L}_A(g \cdot \mathbf{w}) = \mathbf{w}^T A^{\frac{1}{2}T} \rho(g)^T A^{-\frac{1}{2}T} A A^{-\frac{1}{2}} \rho(g) A^{\frac{1}{2}} \mathbf{w} = \mathbf{w}^T A \mathbf{w} = \mathcal{L}_A(\mathbf{w}). \quad (16)$$

Let $S_c = \{\mathbf{w} : \mathcal{L}_A(\mathbf{w}) = c\}$ be a level set of \mathcal{L}_A . We show that after a teleportation, every point on the gradient flow trajectory is optimal in its level set (with full proof in Appendix C.3).

Proposition 5.5. *If at point \mathbf{w} , $\|\nabla \mathcal{L}_A|_{\mathbf{w}}\|^2$ is at a maximum in $S_{\mathcal{L}_A(\mathbf{w})}$, then for any point \mathbf{w}' on the gradient flow trajectory starting from \mathbf{w} , $\|\nabla \mathcal{L}_A|_{\mathbf{w}'}\|^2$ is at a maximum in $S_{\mathcal{L}_A(\mathbf{w}')}$.*

Finally, we observe that for \mathcal{L}_A , teleportation moves the parameters closer to the global minimum in Euclidean distance. In other words, maximizing the magnitude of gradient minimizes the distance to \mathbf{w}^* in a loss level set.

Proposition 5.6. *Consider a point \mathbf{w} in the parameter space. Let $g = \arg \max_{g \in G} \|\nabla \mathcal{L}_A|_{g \cdot \mathbf{w}}\|^2$. Then $g \cdot \mathbf{w} = \arg \min_{\mathbf{w}' \in S_{\mathcal{L}_A(\mathbf{w})}} \|\mathbf{w}' - \mathbf{w}^*\|_2^2$.*

5.4 Relation to second-order optimization methods

Since our algorithm involves optimizing the gradients, symmetry teleportation is closely related to second-order optimization methods. At the target point to teleport to, gradient descent becomes equivalent to Newton's method (proof in Appendix C.4).

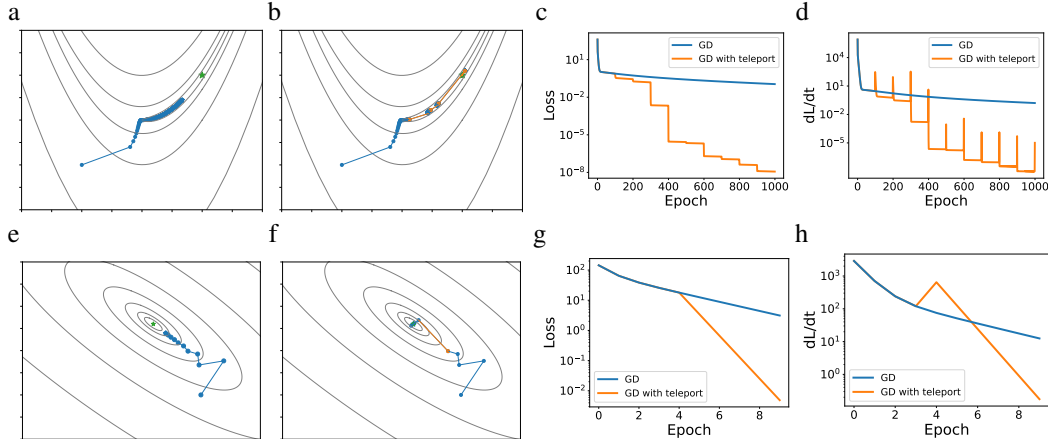


Figure 2: Optimization of the Rosenbrock function (top row) and Booth function (bottom row) using (a) gradient descent and (b) the proposed algorithm. Contours represent the level sets of the loss function. Loss \mathcal{L} and convergence rate $d\mathcal{L}/dt$ are shown in (c) and (d). Teleportation helps move the parameters towards the target.

Proposition 5.7. *Let $S_{\mathcal{L}_0} = \{\mathbf{w} : \mathcal{L}(\mathbf{w}) = \mathcal{L}_0\}$ be a level set of \mathcal{L} . If at a particular $\mathbf{w} \in S_{\mathcal{L}_0}$ we have $\|\nabla\mathcal{L}(\mathbf{w})\|_2 \geq \|\nabla\mathcal{L}(\mathbf{w}')\|_2$ for all \mathbf{w}' in a small neighborhood of \mathbf{w} in $S_{\mathcal{L}_0}$, then the gradient $\nabla\mathcal{L}(\mathbf{w})$ has the same direction as the direction from Newton’s method, $H^{-1}\nabla\mathcal{L}(\mathbf{w})$.*

Proposition 5.7 provides an alternative way to interpret teleportation. Instead of computing the Newton’s direction, we search within the loss level set for a point where the gradient has the same direction as Newton’s direction. However, symmetry teleportation does not require computing the full Hessian matrix. The second derivative required for optimizing over continuous groups is obtained by taking derivatives with respect to parameters and then with respect to the group element, as opposed to taking the derivative with respect to parameters twice. This makes the computation significantly more feasible than Newton’s method on neural networks with large number of parameters.

In practice, however, the group action used for teleportation is usually not transitive. Additionally, we do not teleport using the optimal group element since it can be unbounded. We also do not apply teleportation in every gradient descent step. Therefore, Proposition 5.7 serves as an intuition instead of an exact formulation of how teleportation works. We provide empirical evidence in Section 6 that these approximations do not erase the benefits of teleportation completely, and leave theoretical investigations of the connection to second-order methods under approximations as future work.

6 Experiments

6.1 Acceleration through symmetry teleportation

We examine the effect of symmetry teleportation on optimization. We illustrate teleportation in the parameter space on two test functions and show a speedup in regression and classification problems using multilayer neural networks. For test functions, we compared with GD for illustration purposes. For multi-layer neural networks, we also include AdaGrad as a more competitive baseline.

Rosenbrock function. We apply symmetry teleportation to optimize the 2-variable Rosenbrock function (3). The parameters x_1, x_2 are initialized to $(-1, -1)$. Each algorithm is run 1000 steps with learning rate 10^{-3} . We teleport the parameters every 100 steps. The group elements are found by gradient ascent on θ , the parameter for the $SO(2)$ group, for 10 steps with learning rate 10^{-1} .

The trajectory of parameters and the loss level sets are plotted in Figure 2a,b. The blue star denotes the final position of parameters, the green star denotes the target, and orange dots are the positions from which symmetry teleportation transforms start. While gradient descent is not able to reach the target in 1000 steps, teleportation allows large steps and reaches the target much earlier. Figure 2d shows that

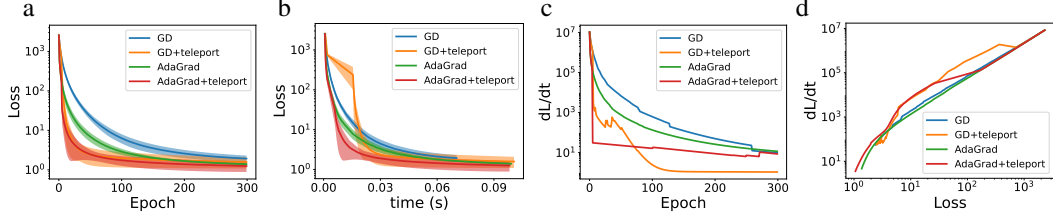


Figure 3: Multi-layer network optimization using gradient descent with and without teleportation. Teleportation reduces both the number of epochs and the total computational time required to reach convergence. At the same loss values, the teleported version has a larger gradient.

teleportation improves the norm of gradients in the following step, and 2c shows its effect on the loss value. Teleportations clearly reduce the number of steps needed for convergence.

Booth function. We also test symmetry teleportation on the Booth function defined in Eqn. (4). We initialize the parameters x_1, x_2 to $(5, -5)$. Each algorithm is run 10 steps with learning rate 0.08. We perform symmetry teleportation on the parameters once, before epoch 5. The group elements are found by gradient ascent on θ for 10 steps with learning rate 0.001. θ is initialized uniformly at random over $[0, \pi)$. Similar to the Rosenbrock function, teleportation moves the parameters to a trajectory with a larger convergence rate (Figure 2 bottom row).

Multilayer neural network regression. We further evaluated our method on a three-layer neural network with a regression loss $\min_{W_1, W_2, W_3} \|Y - W_3 \sigma(W_2 \sigma(W_1 X))\|_2$. The dimension of weight matrices are $W_3 \in \mathbb{R}^{8 \times 7}$, $W_2 \in \mathbb{R}^{7 \times 6}$, and $W_1 \in \mathbb{R}^{6 \times 5}$. $X \in \mathbb{R}^{5 \times 4}$ is the data, $Y \in \mathbb{R}^{8 \times 4}$ is the target, and σ is the LeakyReLU activation with slope coefficient 0.1. Additional hyperparameter details can be found in Appendix D.2.

Teleportation of the $GL(\mathbb{R})$ group can be performed by finding an element x in its Lie algebra, such that transforming w by the group element $g = \exp(x)$ improves the gradient $\frac{d\mathcal{L}}{dt}$. We use the first order approximation of the exponential map. Between each pair of weight matrices, we replace g_m by $I + T$ and g_m^{-1} by $I - T$ in (8), where $T \in \mathbb{R}^{d_m \times d_m}$ is initialized to 0. Then we perform gradient ascent steps on T with objective defined in Line 3 of Algorithm 1 and update the pair of weights.

Figure 3a and 3b show the training curves plotted against epochs and time. Shaded area denotes one standard deviation from 5 runs. Since GD and AdaGrad use different learning rates, they are not directly comparable. However, the addition of teleportation clearly improves both algorithms. Figure 3c and 3d shows the squared norm of gradient from a single run. Teleportation increases the magnitude of gradient, and the trajectory with teleportation has a larger $d\mathcal{L}/dt$ value at the same loss values, which demonstrates that teleportation finds a better trajectory.

MNIST classification. We apply symmetry teleportation on the MNIST classification task (Deng, 2012). We split the training set into 48,000 for training and 12,000 for validation. The input data has dimension 28×28 and is flattened into a vector. The output of the neural network has dimension 10 corresponding to the 10 digit classes. We used a three-layer neural network with hidden dimension $[512, 512]$, LeakyReLU activations, and cross-entropy loss. Learning rate is 2×10^{-3} , and learning rate for teleportation is 10^{-3} . Each optimization algorithm is run 80 epochs with batch size of 20. Immediately after the first epoch, we apply teleportation using data from one mini-batch, and repeat for 4 different mini-batches. For each mini-batch, 10 gradient ascent steps are used to optimize g_m .

Figure 4a,b shows the effect of teleportation on training and validation loss, and Figure 4c,d shows the norm of the gradient in training. While teleportation significantly accelerates the decrease of the training loss in SGD, its effect on the validation loss is limited and detrimental for AdaGrad. Therefore, teleportation on MNIST makes training faster at the beginning but leads to earlier overfit and slightly worse validation accuracy. A possible reason is that regions with large gradients have sharp minima that do not generalize well.

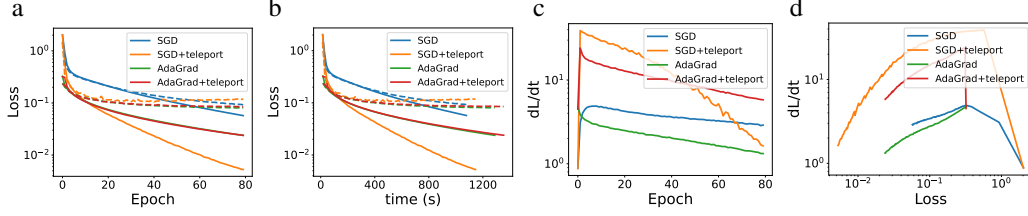


Figure 4: MNIST classification using gradient descent with and without teleportation. Solid lines are training loss and dashed lines are validation loss.

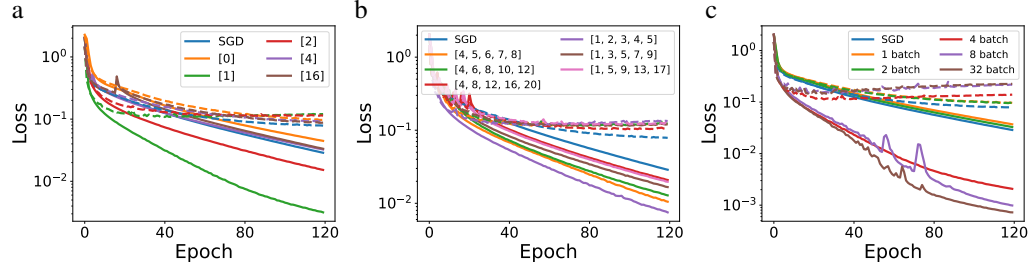


Figure 5: Teleportation (a) once at different epoch, (b) 5 times with different teleportation schedules, and (c) using different number of mini-batches. The lists in the legend of (a) and (c) denote the epoch numbers in teleportation schedule where teleportation happens.

6.2 Teleportation schedule

The effect of teleportation varies depending on its time and frequency. Figure 5 shows the result of teleportation on MNIST with different hyperparameters. In all experiments, we use SGD with batch size 20 , learning rate 2×10^{-3} , and 10 gradient ascent steps for each teleportation.

In Figure 5a, we randomly select 4 different mini-batches and apply teleportation on each of them individually, but at different epochs. Teleportation before training has the worst performance. After epoch 0, the effect of teleportation is stronger when it is applied earlier. In Figure 5b, we again apply teleportations on 4 randomly selected mini-batches, but repeat this with 5 different teleportation schedules (hyperparameter K in Algorithm 2) as shown in the legend. All schedules have the same number of teleportations. Smaller intervals between teleportations accelerate convergence more significantly. In Figure 5c, we apply teleportation immediately after the first epoch, but use different numbers of mini-batches (hyperparameter B in Algorithm 2) and teleport using each of them individually. Using more mini-batches to teleport leads to faster decrease in training loss but is also more prone to overfitting.

6.3 Runtime analysis

The additional amount of computation introduced by teleportation depends on the implementation of Line 2-5 of Algorithm 1. We discuss our implementation for teleporting multi-layer neural networks as an example. Teleporting each pair of adjacent weight matrices requires computing the inverse of the output from the previous layer. Denote the batch size as n , the largest dimension of all layers as d_{max} , and the number of layers as l . Assume that $d_{max} > n$. Computing the inverse of the output of each layer has complexity $O(d_{max}^2 n)$, and computing the pseudoinverse for all layers has complexity $O(d_{max}^2 nl)$. Note that all matrices we invert have dimensions at most $d_{max} \times n$.

For one gradient ascent step on g , the forward and backward pass both have complexity $O(d_{max}^2 nl)$. This is the same as the forward and backward pass of gradient descent on w because the architecture is the same except with approximately twice as many layers. We perform t gradient ascent steps on g . Therefore, the computation cost for one teleportation is $O(d_{max}^2 nlt)$.

We show empirically that the runtime for teleportation scales polynomially with matrix dimensions and linearly with the number of layers. We record the runtime of gradient descent on a Leaky-ReLU neural network for 300 epochs, with a 10-step teleportation every 10 epochs. Each pair of adjacent weight matrices is transformed by a group action during teleportation. Figure 6(a) shows the runtime

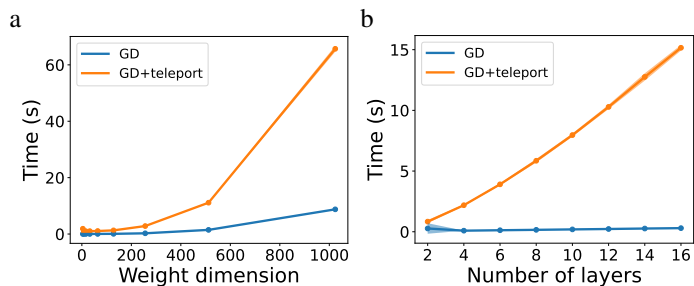


Figure 6: Gradient descent training time on a Leaky-ReLU neural network for 300 epochs, with a 10-step teleportation every 10 epochs. (a) 3-layer network using square weights and data matrices, with different dimensions. (b) Weights and data are all 128 by 128 matrices, but the network has different number of layers.

for a 3-layer network using square weights and data matrices with different dimensions. Figure 6(b) shows the runtime for 128-by-128 weight and data matrices with different number of layers.

Although the teleportation step has the same complexity as a gradient descent step, the runtime is dominated by teleportation due to larger constants in the complexity analysis. The trade-off between teleportation time and convergence rate depends on specific problems. In our experiments, the convergence rate is improved by a small number of teleportation steps which does not add significant computational overhead.

7 Discussion and Conclusions

We proposed a new optimization algorithm that exploits the symmetry in the loss landscape to improve convergence. It is interesting to note that optimizing $d\mathcal{L}/dt$ locally sometimes leads to an improved global path. One example is the ellipse function (Figure 1), where teleporting once ensures that $d\mathcal{L}/dt$ is optimal at every \mathcal{L} value along the trajectory. Another example is the matrix factorization problem $\mathcal{L}(U, V) = \|Y - UV\|_2^2$. Tarmoun et al. (2021) shows that the convergence rate increases with the imbalance $U^T U - V^T V$. Consider the transformation $U, V \rightarrow Ug, g^{-1}V$. To optimize $d\mathcal{L}(U, V)/dt$ locally, we would need a large $g \in \text{GL}_n$, but a large g also leads to a large $U^T U - V^T V$ which is positively correlated with the overall convergence rate of the entire trajectory. Hence teleportation is guaranteed to produce a better trajectory.

A potential future direction is to derive the exact expression for how teleportation affects the loss value at a later time in gradient flow, which may lead to a closed-form solution of the optimal teleportation destination. Additionally, inspired by the landscape view of parameter space symmetry Şimşek et al. (2021), teleportation using discrete (permutation) symmetries may allow us to reach a better minimum. Finally, additional theory can be developed to explain the relationship between teleportation and second-order methods under the approximations we introduced, especially to quantify the improvement on the overall convergence rate, and to derive its effect on generalization bounds. Integrating teleportation with other advanced optimizers such as Adam and RMSprop would be another interesting future step.

Acknowledgments and Disclosure of Funding

This work was supported in part by U.S. Department Of Energy, Office of Science, U. S. Army Research Office under Grant W911NF-20-1-0334, Google Faculty Award, Amazon Research Award, and NSF Grants #2134274, #2107256 and #2134178. R. Walters is supported by the Roux Institute and the Harold Alfond Foundation. We are grateful to Iordan Ganev for many helpful discussions.

References

Shun-Ichi Amari. Natural gradient works efficiently in learning. *Neural computation*, 10(2):251–276, 1998.

- Marco Armenta and Pierre-Marc Jodoin. The representation theory of neural networks. *Mathematics*, 9(24), 2021. ISSN 2227-7390.
- Marco Armenta, Thierry Judge, Nathan Painchaud, Youssef Skandarani, Carl Lemaire, Gabriel Gibeau Sanchez, Philippe Spino, and Pierre-Marc Jodoin. Neural teleportation. *arXiv preprint arXiv:2012.01118*, 2020.
- Sanjeev Arora, Nadav Cohen, and Elad Hazan. On the optimization of deep networks: Implicit acceleration by overparameterization. In *International Conference on Machine Learning*, pages 244–253. PMLR, 2018.
- Thomas Back. *Evolutionary algorithms in theory and practice: evolution strategies, evolutionary programming, genetic algorithms*. Oxford university press, 1996.
- Vijay Badrinarayanan, Bamdev Mishra, and Roberto Cipolla. Symmetry-invariant optimization in deep networks. *arXiv preprint arXiv:1511.01754*, 2015.
- Robert Bamler and Stephan Mandt. Improving optimization for models with continuous symmetry breaking. In *International Conference on Machine Learning*, pages 423–432. PMLR, 2018.
- Mikhail Belkin, Daniel Hsu, Siyuan Ma, and Soumik Mandal. Reconciling modern machine-learning practice and the classical bias–variance trade-off. *Proceedings of the National Academy of Sciences*, 116(32):15849–15854, 2019.
- Patrick L Combettes and Jean-Christophe Pesquet. Proximal splitting methods in signal processing. In *Fixed-point algorithms for inverse problems in science and engineering*, pages 185–212. Springer, 2011.
- Li Deng. The MNIST database of handwritten digit images for machine learning research. *IEEE Signal Processing Magazine*, 29(6):141–142, 2012.
- Simon S Du, Wei Hu, and Jason D Lee. Algorithmic regularization in learning deep homogeneous models: Layers are automatically balanced. *Neural Information Processing Systems*, 2018.
- John Duchi, Elad Hazan, and Yoram Singer. Adaptive subgradient methods for online learning and stochastic optimization. *Journal of machine learning research*, 12(7), 2011.
- Jordan Ganev, Twan van Laarhoven, and Robin Walters. Universal approximation and model compression for radial neural networks. *arXiv preprint arXiv:2107.02550*, 2021.
- Grzegorz Gluch and Rüdiger Urbanke. Noether: The more things change, the more stay the same. *arXiv preprint arXiv:2104.05508*, 2021.
- Vineet Gupta, Tomer Koren, and Yoram Singer. Shampoo: Preconditioned stochastic tensor optimization. In *35th International Conference on Machine Learning*, 2018.
- Elad Hazan. Lecture notes: Optimization for machine learning. *arXiv preprint arXiv:1909.03550*, 2019.
- Momin Jamil and Xin-She Yang. A literature survey of benchmark functions for global optimisation problems. *International Journal of Mathematical Modelling and Numerical Optimisation*, 4(2): 150–194, 2013.
- Diederik P Kingma and Jimmy Ba. Adam: A method for stochastic optimization. *International Conference on Learning Representations*, 2015.
- Daniel Kunin, Javier Sagastuy-Brena, Surya Ganguli, Daniel LK Yamins, and Hidenori Tanaka. Neural mechanics: Symmetry and broken conservation laws in deep learning dynamics. In *International Conference on Learning Representations*, 2021.
- Serge Lang. *Algebra*. Graduate Texts in Mathematics. Springer, 2002. ISBN 978-0387953854.
- James Martens and Roger B Grosse. Optimizing neural networks with kronecker-factored approximate curvature. In *International Conference on International Conference on Machine Learning*. PMLR, 2018.

- Qi Meng, Shuxin Zheng, Huishuai Zhang, Wei Chen, Zhi-Ming Ma, and Tie-Yan Liu. \mathcal{G} -SGD: Optimizing relu neural networks in its positively scale-invariant space. *International Conference on Learning Representations*, 2019.
- Hancheng Min, Salma Tarmoun, René Vidal, and Enrique Mallada. On the explicit role of initialization on the convergence and implicit bias of overparametrized linear networks. In *International Conference on Machine Learning*. PMLR, 2021.
- Behnam Neyshabur, Russ R Salakhutdinov, and Nati Srebro. Path-SGD: Path-normalized optimization in deep neural networks. In *Advances in Neural Information Processing Systems*, 2015.
- HoHo Rosenbrock. An automatic method for finding the greatest or least value of a function. *The Computer Journal*, 3(3):175–184, 1960.
- Andrew M. Saxe, James L. McClelland, and Surya Ganguli. Exact solutions to the nonlinear dynamics of learning in deep linear neural networks. *International Conference on Learning Representations*, 2014.
- Berfin Şimşek, François Ged, Arthur Jacot, Francesco Spadaro, Clément Hongler, Wulfram Gerstner, and Johanni Brea. Geometry of the loss landscape in overparameterized neural networks: Symmetries and invariances. In *International Conference on Machine Learning*, pages 9722–9732. PMLR, 2021.
- Salma Tarmoun, Guilherme Franca, Benjamin D Haeffele, and Rene Vidal. Understanding the dynamics of gradient flow in overparameterized linear models. In *International Conference on Machine Learning*, pages 10153–10161. PMLR, 2021.
- Twan Van Laarhoven. L2 regularization versus batch and weight normalization. *Advances in Neural Information Processing Systems*, 2017.

A Adaptations of Algorithm 1 for different problems

A.1 Stochastic gradient descent

We extend Algorithm 1 to stochastic gradient descent (SGD). We apply the group actions using data from a mini-batch X_i , and repeat for B mini-batches each time. The gradient we optimize, $\tilde{\nabla}\mathcal{L}(X_i, g \cdot \mathbf{w}_t)$, also uses single mini-batches. Algorithm 2 provides the framework for teleportation in SGD.

Algorithm 2: Symmetry Teleportation (SGD)

Input: Loss function $\mathcal{L}(\mathbf{w})$, learning rate η , number of epochs t_{max} , initialized parameters \mathbf{w}_0 , symmetry group G , teleportation schedule K , number of mini-batches used to teleport B .

Output: $\mathbf{w}_{t_{max}}$.

```

1 for  $t \leftarrow 0$  to  $t_{max} - 1$  do
2   if  $t \in K$  then
3     for  $X_i$  in the first  $B$  mini-batches do
4        $g \leftarrow \operatorname{argmax}_{g \in G} \|\tilde{\nabla}\mathcal{L}(X_i, g \cdot \mathbf{w}_t)\|^2$ 
5        $\mathbf{w}_t \leftarrow g \cdot \mathbf{w}_t$ 
6        $\mathbf{w}_t \leftarrow \mathbf{w}_t - \eta \tilde{\nabla}\mathcal{L}(X_i, \mathbf{w}_t)$ 
7     end for
8     for  $X_i$  in the rest mini-batches do
9        $\mathbf{w}_t \leftarrow \mathbf{w}_t - \eta \tilde{\nabla}\mathcal{L}(X_i, \mathbf{w}_t)$ 
10    end for
11  else
12    for all mini-batches  $X_i$  do
13       $\mathbf{w}_t \leftarrow \mathbf{w}_t - \eta \tilde{\nabla}\mathcal{L}(X_i, \mathbf{w}_t)$ 
14    end for
15  end if
16   $\mathbf{w}_{t+1} \leftarrow \mathbf{w}_t$ 
17 end for
18 return  $\mathbf{w}_{t_{max}}$ 

```

A.2 Data transformation

Algorithm 3 here modifies Algorithm 1 to allow transformations on both parameters and data. Denote g_X as the group action on data only. The group actions on data at all teleportation steps can be precomposed as a function f and applied to the input data at inference time.

Algorithm 3: Symmetry Teleportation (with data transformation)

Input: Loss function $\mathcal{L}(\mathbf{w}, X)$, learning rate η , number of epochs t_{max} , initialized parameters \mathbf{w}_0 , symmetry G , teleportation schedule K , data X .

Output: $\mathbf{w}_{t_{max}}$, data transformation f .

Initialize: $f =$ the identity function.

```

1 for  $t \leftarrow 0$  to  $t_{max} - 1$  do
2   if  $t \in K$  then
3      $g \leftarrow \operatorname{argmax}_{g \in G} \|\nabla_{g \cdot \mathbf{w}_t} \mathcal{L}(g \cdot (\mathbf{w}_t, X))\|^2$ 
4      $\mathbf{w}_t, X \leftarrow g \cdot (\mathbf{w}_t, X)$ 
5      $f \leftarrow g_X \circ f$ 
6   end if
7    $\mathbf{w}_{t+1} \leftarrow \mathbf{w}_t - \eta \nabla_{\mathbf{w}_t} \mathcal{L}$ 
8 end for
9 return  $\mathbf{w}_{t_{max}}, f$ 

```

B Group actions

In this section, we derive the group actions for the test functions and multi-layer neural networks. More details about group theory can be found in textbooks such as Lang (2002).

B.1 Continuous symmetry in test functions

B.1.1 Ellipse

Consider the following loss function with $a \in \mathbb{R}^{\geq 0}$:

$$\mathcal{L}(x_1, x_2) = x_1^2 + ax_2^2 \quad (17)$$

If we change the variables to $\mathcal{L}(u(x_1, x_2), v(x_1, x_2)) = u^2 + v^2$, 2D rotations leave \mathcal{L} unchanged. Therefore $SO(2)$ is a symmetry of $\mathcal{L}(x_1, x_2)$. Let $g_\theta \in SO(2)$, and define the group action as

$$g_\theta \cdot \begin{bmatrix} x_1 \\ x_2 \end{bmatrix} = \begin{bmatrix} 1 & 0 \\ 0 & 1/\sqrt{a} \end{bmatrix} \begin{bmatrix} \cos \theta & -\sin \theta \\ \sin \theta & \cos \theta \end{bmatrix} \begin{bmatrix} 1 & 0 \\ 0 & \sqrt{a} \end{bmatrix} \begin{bmatrix} x_1 \\ x_2 \end{bmatrix} \quad (18)$$

Then

$$\mathcal{L}(x_1, x_2) = \mathcal{L}(g \cdot (x_1, x_2)) \quad (19)$$

B.1.2 Rosenbrock function

Consider the Rosenbrock function with 2 variables Rosenbrock (1960):

$$\mathcal{L}(x_1, x_2) = 100(x_1^2 - x_2)^2 + (x_1 - 1)^2 \quad (20)$$

Let $u = 10(x_1^2 - x_2)$ and $v = x_1 - 1$. After changing the variables from x and y to u and v , \mathcal{L} has a rotational symmetry. Note that the function, $h : \mathbb{R}^2 \rightarrow \mathbb{R}^2$, that maps x_1, x_2 to u, v is bijective:

$$\begin{aligned} (u, v) &= h(x_1, x_2) = (10(x_1^2 - x_2), x_1 - 1) \\ (x_1, x_2) &= h^{-1}(u, v) = (v + 1, (v + 1)^2 - 0.1u) \\ h(x_1, x_2) &= h(y_1, y_2) \Rightarrow (x_1, x_2) = (y_1, y_2) \end{aligned} \quad (21)$$

Next, we show that $SO(2)$ is a symmetry of $\mathcal{L}(x_1, x_2)$. Let ρ be a representation of $SO(2)$ acting on \mathbb{R}^2 . For $g \in SO(2)$, define the following group action:

$$g \cdot (x_1, x_2) = h^{-1}(\rho(g)h(x_1, x_2)) \quad (22)$$

Then

$$\mathcal{L}(x_1, x_2) = \mathcal{L}(g \cdot (x_1, x_2)) \quad (23)$$

For the Rosenbrock function with $2N$ parameters, we can construct a bijective function $h : \mathbb{R}^{2N} \rightarrow \mathbb{R}^{2N}$ by transforming each of the N pairs of variables as before, and $SO(2N)$ is a symmetry of $\mathcal{L}(x_1, \dots, x_{2N})$. However, we will only use the 2 variable version in the experiments.

B.1.3 Booth function

Consider the Booth function Jamil and Yang (2013):

$$\mathcal{L}(x_1, x_2) = (x_1 + 2x_2 - 7)^2 + (2x_1 + x_2 - 5)^2$$

Similar to the Rosenbrock function, a change of variables reveals a rotational symmetry of \mathcal{L} :

$$\begin{aligned} (u, v) &= h(x_1, x_2) = (x_1 + 2x_2 - 7, 2x_1 + x_2 - 5) \\ (x_1, x_2) &= h^{-1}(u, v) = \left(-\frac{1}{3}u + \frac{2}{3}v + 1, \frac{2}{3}u - \frac{1}{3}v + 3\right) \end{aligned} \quad (24)$$

The function $h : \mathbb{R}^2 \rightarrow \mathbb{R}^2$ that maps x_1, x_2 to u, v is bijective. Let ρ be a representation of $SO(2)$ acting on \mathbb{R}^2 . For $g \in SO(2)$, define the following group action:

$$g \cdot (x_1, x_2) = h^{-1}(\rho(g)h(x_1, x_2)) \quad (25)$$

Then $\mathcal{L}(x_1, x_2)$ admits an $SO(2)$ symmetry:

$$\mathcal{L}(x_1, x_2) = \mathcal{L}(g \cdot (x_1, x_2)) \quad (26)$$

B.2 Continuous symmetry in multi-layer neural Networks

In this and the following sections, we provide proofs for the theoretical results. We restate the propositions from the main text for readability.

Proposition 4.2. *A linear network is invariant under all groups $G_m \equiv \text{GL}_{d_m}$ acting as*

$$g \cdot (W_m, W_{m-1}) = (W_m g^{-1}, g W_{m-1}), \quad g \cdot W_k = W_k, \quad \forall k \notin \{m, m-1\}.$$

Proof. In the linear network $h_m = W_m h_{m-1}$, hence

$$g \cdot (W_m, h_{m-1}) = (W_m g^{-1}, g h_{m-1}), \quad g \cdot h_m = W_m g^{-1} g h_{m-1} = h_m \quad (27)$$

which means a p -layer linear network is invariant under all G_m with $m \leq p$ as they keep the output h_p invariant ($\forall g \in G_m, g \cdot h_p = h_p$). \square

Proposition 4.3. *Assume that h_{m-2} is invertible. A multi-layer network with bijective activation σ has a $\text{GL}_{d_{m-1}}$ symmetry. For $g_m \in G_m = \text{GL}_{d_{m-1}}(\mathbb{R})$ the following group action keeps h_p with $p \geq m$ invariant*

$$g_m \cdot W_k = \begin{cases} W_m g_m^{-1} & k = m \\ \sigma^{-1}(g_m \sigma(W_{m-1} h_{m-2})) h_{m-2}^{-1} & k = m-1 \\ W_k & k \notin \{m, m-1\} \end{cases} \quad (28)$$

Proof. From (7), we want to convert $g \cdot h_{m-1}$ into a transformation on W_{m-1} instead of h_{m-1} . In other words, we want to find a set of transformed weights W'_m, W'_{m-1} which yields the same network output \tilde{h}_m :

$$\begin{aligned} \tilde{h}_m &= W'_m \sigma(W'_{m-1} h_{m-2}) = W_m g^{-1} g \sigma(W_{m-1} h_{m-2}) \\ \Rightarrow W'_m &= W_m g^{-1}, \quad \sigma(W'_{m-1} h_{m-2}) = g \sigma(W_{m-1} h_{m-2}) \end{aligned} \quad (29)$$

Solving (29) we get

$$W'_{m-1} = \sigma^{-1}(g \sigma(W_{m-1} h_{m-2})) h_{m-2}^{-1}. \quad (30)$$

(28) follows from (29) and (30).

To verify that (28) is a valid group action,

$$\begin{aligned} I \cdot W_k &= \begin{cases} W_m I & k = m \\ \sigma^{-1}(I \sigma(W_{m-1} h_{m-2})) h_{m-2}^{-1} & k = m-1 \\ W_k & k \notin \{m, m-1\} \end{cases} \\ &= W_k \end{aligned} \quad (31)$$

and

$$\begin{aligned} g_1 \cdot (g_2 \cdot W_k) &= \begin{cases} W_m g_2^{-1} g_1^{-1} & k = m \\ \sigma^{-1}(g_1 \sigma([\sigma^{-1}(g_2 \sigma(W_{m-1} h_{m-2})) h_{m-2}^{-1}] h_{m-2})) h_{m-2}^{-1} & k = m-1 \\ W_k & k \notin \{m, m-1\} \end{cases} \\ &= \begin{cases} W_m (g_1 g_2)^{-1} & k = m \\ \sigma^{-1}((g_1 g_2) \sigma(W_{m-1} h_{m-2})) h_{m-2}^{-1} & k = m-1 \\ W_k & k \notin \{m, m-1\} \end{cases} \\ &= (g_1 g_2) \cdot W_k \end{aligned} \quad (32)$$

\square

C Theoretical analysis of teleportation

C.1 What symmetries help accelerate optimization

Proposition 5.1. *Let $\mathbf{w}' = g \cdot \mathbf{w}$ be a point we teleport to. Let $J = \partial \mathbf{w}' / \partial \mathbf{w}$ be the Jacobian. Symmetry teleportation using g accelerates the rate of decay in \mathcal{L} if it satisfies*

$$\left\| [J^{-1}]^T \nabla \mathcal{L}(\mathbf{w}) \right\|_{\eta}^2 > \|\nabla \mathcal{L}(\mathbf{w})\|_{\eta}^2.$$

Proof. Let $\mathbf{w}' = g \cdot \mathbf{w}$. Denote the Jacobian as J , where $J_{ij} = \partial w'_i / \partial w_j$. Then the inverse of J has entries $J_{ij}^{-1} = \partial w_i / \partial w'_j$.

The gradient at \mathbf{w}' is

$$\frac{\partial \mathcal{L}(\mathbf{w}')}{\partial \mathbf{w}'} = \frac{\partial \mathcal{L}(\mathbf{w})}{\partial \mathbf{w}'} = \sum_j \frac{\partial \mathcal{L}(\mathbf{w})}{\partial w_j} \frac{\partial w_j}{\partial w'_i} = \sum_j \frac{\partial \mathcal{L}(\mathbf{w})}{\partial w_j} J_{ji}^{-1} = \left(\left(\frac{\partial \mathcal{L}(\mathbf{w})}{\partial \mathbf{w}} \right)^T J^{-1} \right)^T = (J^{-1})^T \frac{\partial \mathcal{L}(\mathbf{w})}{\partial \mathbf{w}} \quad (33)$$

The rate of change of \mathcal{L} in gradient flow is

$$\frac{d\mathcal{L}(\mathbf{w}')}{dt} = \left\langle \frac{\partial \mathcal{L}}{\partial \mathbf{w}'}, \frac{d\mathbf{w}'}{dt} \right\rangle = - \left\| (J^{-1})^T \frac{\partial \mathcal{L}(\mathbf{w})}{\partial \mathbf{w}} \right\|_{\eta}^2 \quad (34)$$

Thus we will have a speedup if

$$\left\| (J^{-1})^T \frac{\partial \mathcal{L}(\mathbf{w})}{\partial \mathbf{w}} \right\|_{\eta}^2 > \left\| \frac{\partial \mathcal{L}(\mathbf{w})}{\partial \mathbf{w}} \right\|_{\eta}^2 \quad (35)$$

□

Proof of Corollary 5.2

Proof. Since $J = g$, using (9) and the l.h.s. of (10) we have

$$\frac{d\mathcal{L}(g \cdot \mathbf{w})}{dt} = -\nabla \mathcal{L}^T g^{-1} \eta [g^{-1}]^T \nabla \mathcal{L} = \nabla \mathcal{L}^T [g^T \eta^{-1} g]^{-1} \nabla \mathcal{L} = \|\nabla \mathcal{L}\|_{\eta}^2 \quad (36)$$

□

C.2 Improvement of subsequent steps

Proposition 5.4. *Consider the gradient descent with a G -invariant loss $\mathcal{L}(\mathbf{w})$ and learning rate $\eta \in \mathbb{R}^+$. Let \mathbf{w}_t be the parameter at time t and $\mathbf{w}'_t = g \cdot \mathbf{w}_t$ the parameter teleported by $g \in G$. Let \mathbf{w}_{t+T} and \mathbf{w}'_{t+T} be the parameters after T more steps of gradient descent from \mathbf{w}_t and \mathbf{w}'_t respectively. Under Assumption 5.3, if $\eta L < 1$, and*

$$\frac{\|\partial \mathcal{L} / \partial \mathbf{w}'_t\|_2}{\|\partial \mathcal{L} / \partial \mathbf{w}_t\|_2} \geq \frac{(1 + \eta L)^T}{(1 - \eta L)^T},$$

then

$$\left\| \frac{\partial \mathcal{L}}{\partial \mathbf{w}'_{t+T}} \right\|_2 \geq \left\| \frac{\partial \mathcal{L}}{\partial \mathbf{w}_{t+T}} \right\|_2.$$

Proof. From the definition of Lipschitz continuity and the update rule of gradient descent,

$$\left| \left\| \frac{\partial \mathcal{L}}{\partial \mathbf{w}_{t+1}} \right\|_2 - \left\| \frac{\partial \mathcal{L}}{\partial \mathbf{w}_t} \right\|_2 \right| \leq L \|\mathbf{w}_{t+1} - \mathbf{w}_t\|_2 = L \left\| \eta \frac{\partial \mathcal{L}}{\partial \mathbf{w}_t} \right\|_2 \quad (37)$$

Equivalently,

$$(1 - \eta L) \left\| \frac{\partial \mathcal{L}}{\partial \mathbf{w}_t} \right\|_2 \leq \left\| \frac{\partial \mathcal{L}}{\partial \mathbf{w}_{t+1}} \right\|_2 \leq (1 + \eta L) \left\| \frac{\partial \mathcal{L}}{\partial \mathbf{w}_t} \right\|_2 \quad (38)$$

By unrolling T steps, we have

$$(1 - \eta L)^T \left\| \frac{\partial \mathcal{L}}{\partial \mathbf{w}_t} \right\|_2 \leq \left\| \frac{\partial \mathcal{L}}{\partial \mathbf{w}_{t+T}} \right\|_2 \leq (1 + \eta L)^T \left\| \frac{\partial \mathcal{L}}{\partial \mathbf{w}_t} \right\|_2 \quad (39)$$

Similarly, for a teleported point $\mathbf{w}'_t = g \cdot \mathbf{w}_t$,

$$(1 - \eta L)^T \left\| \frac{\partial \mathcal{L}}{\partial \mathbf{w}'_t} \right\|_2 \leq \left\| \frac{\partial \mathcal{L}}{\partial \mathbf{w}'_{t+T}} \right\|_2 \leq (1 + \eta L)^T \left\| \frac{\partial \mathcal{L}}{\partial \mathbf{w}'_t} \right\|_2 \quad (40)$$

Therefore, if

$$(1 - \eta L)^T \left\| \frac{\partial \mathcal{L}}{\partial \mathbf{w}'_t} \right\|_2 \geq (1 + \eta L)^T \left\| \frac{\partial \mathcal{L}}{\partial \mathbf{w}_t} \right\|_2 \quad (41)$$

then it is guaranteed that

$$\left\| \frac{\partial \mathcal{L}}{\partial \mathbf{w}'_{t+T}} \right\|_2 \geq \left\| \frac{\partial \mathcal{L}}{\partial \mathbf{w}_{t+T}} \right\|_2 \quad (42)$$

□

C.3 Convergence analysis for convex quadratic functions

We first show that starting from a point in S_c , all other points in S_c can be reached with one teleportation.

Proposition C.1. S_c contains a single orbit. That is, $G \cdot \mathbf{w} \equiv \{g \cdot \mathbf{w} : g \in G\} = S_c$ for all $\mathbf{w} \in S_c$.

Proof. Consider two points $\mathbf{w}_1, \mathbf{w}_2 \in S_c$. Then $\mathbf{w}_1^T A \mathbf{w}_1 = (A^{\frac{1}{2}} \mathbf{w}_1)^T (A^{\frac{1}{2}} \mathbf{w}_1) = c$ and $\mathbf{w}_2^T A \mathbf{w}_2 = (A^{\frac{1}{2}} \mathbf{w}_2)^T (A^{\frac{1}{2}} \mathbf{w}_2) = c$. Let $\mathbf{v}_1 = \frac{A^{\frac{1}{2}} \mathbf{w}_1}{\sqrt{c}}$, $\mathbf{v}_2 = \frac{A^{\frac{1}{2}} \mathbf{w}_2}{\sqrt{c}}$ and $\mathbf{e}_1 = [1, 0, \dots, 0]^T$. Since $\|\mathbf{v}_1\| = \|\mathbf{v}_2\| = 1$, there exists $g_1, g_2 \in O(n)$, such that $g_1 \mathbf{e}_1 = \mathbf{v}_1$ and $g_2 \mathbf{e}_1 = \mathbf{v}_2$. One way to construct such g_1 is let the first column be equal to \mathbf{v}_1 and other columns be the rest of the orthonormal basis. Let $g = g_2 g_1^{-1}$. Then $\mathbf{v}_2 = g \mathbf{v}_1$, $A^{\frac{1}{2}} \mathbf{w}_2 = g A^{\frac{1}{2}} \mathbf{w}_1$, and $\mathbf{w}_2 = A^{-\frac{1}{2}} g A^{\frac{1}{2}} \mathbf{w}_1 = g \cdot \mathbf{w}_1$.

We have shown that for any $\mathbf{w}_1, \mathbf{w}_2 \in S_c$, there exists a $g \in G$ such that $\mathbf{w}_2 = g \cdot \mathbf{w}_1$. Therefore, the group action of G on S_c is transitive. Equivalently, S_c contains a single orbit. □

The objective of teleportation is transforming parameters using a group element to maximize the norm of gradient:

$$\max_{g \in G} \|\nabla \mathcal{L}_A|_{g \cdot \mathbf{w}}\|_2^2. \quad (43)$$

Since all points on the level set are reachable, the target teleportation destination is the point with the largest gradient norm on the same level set. In other words, (43) is equivalent to the following optimization problem:

$$\begin{aligned} & \max_{\mathbf{w}'} \|\nabla \mathcal{L}_A|_{\mathbf{w}'}\|_2^2 \\ & \text{s.t. } \mathcal{L}_A(\mathbf{w}') = \mathcal{L}_A(\mathbf{w}). \end{aligned} \quad (44)$$

Let $c = \mathcal{L}_A(\mathbf{w})$. Substitute in \mathcal{L}_A and $\nabla \mathcal{L}_A$, we have the following equivalent formulation:

$$\begin{aligned} & \max_{\mathbf{w}'} \|A \mathbf{w}'\|_2^2 \\ & \text{s.t. } \mathbf{w}'^T A \mathbf{w}' = c. \end{aligned} \quad (45)$$

Next, we solve this optimization problem and show that the gradient norm is maximized on the gradient flow trajectory starting from its solution.

Proposition C.2. *The solution to (45) is an eigenvector of A corresponding to its largest eigenvalue.*

Proof. We solve (45) using the method of Lagrangian multipliers. The Lagrangian of (45) is

$$\mathcal{L} = \mathbf{w}'^T A^T A \mathbf{w}' - \lambda(\mathbf{w}'^T A \mathbf{w}' - c). \quad (46)$$

Setting the derivative with respect of \mathbf{w}' to 0, we have

$$\frac{\partial \mathcal{L}}{\partial \mathbf{w}'} = 2A^T A \mathbf{w}' - 2\lambda A \mathbf{w}' = 0, \quad (47)$$

which gives

$$A^T A \mathbf{w}' = \lambda A \mathbf{w}'. \quad (48)$$

Since A is positive definite, $A = A^T$ and A is invertible. Therefore,

$$A \mathbf{w}' = \lambda \mathbf{w}', \quad (49)$$

so the solution to (45) is an eigenvector of A . Then, the constraint is $\mathbf{w}'^T A \mathbf{w}' = \lambda \|\mathbf{w}'\|^2 = c$, and the objective becomes $\max_{\mathbf{w}'} \lambda^2 \|\mathbf{w}'\|^2 = \max_{\mathbf{w}'} c\lambda$. Therefore, we want λ to be the largest eigenvalue of A . Hence the optimal \mathbf{w}' is an eigenvector of A corresponding to its largest eigenvalue. \square

Proposition 5.5. *If at point \mathbf{w} , $\|\nabla \mathcal{L}_A|_{\mathbf{w}}\|^2$ is at a maximum in $S_{\mathcal{L}_A(\mathbf{w})}$, then for any point \mathbf{w}' on the gradient flow trajectory starting from \mathbf{w} , $\|\nabla \mathcal{L}_A|_{\mathbf{w}'}\|^2$ is at a maximum in $S_{\mathcal{L}_A(\mathbf{w}')}$.*

Proof. From Proposition C.2, \mathbf{w} is an eigenvector of A corresponding to its largest eigenvalue. Then the gradient of \mathcal{L}_A is $A \mathbf{w} = \lambda \mathbf{w}$. Therefore, on the gradient flow trajectory starting from \mathbf{w} , every point has the same direction as \mathbf{w} , meaning that the points are all eigenvectors of A corresponding to its largest eigenvalue. Therefore, $\|\nabla \mathcal{L}_A\|^2$ is always at a maximum on the loss level sets. \square

Finally, we show that maximizing the magnitude of gradient is equivalent to minimizing the distance to \mathbf{w}^* in a loss level set (Proposition 5.6).

Proposition C.3. *The solution to the following optimization problem is the same as the solution to (45):*

$$\begin{aligned} \min_{\mathbf{w}'} \|\mathbf{w}' - \mathbf{w}^*\|_2^2 \\ \text{s.t. } \mathbf{w}'^T A \mathbf{w}' = c. \end{aligned} \quad (50)$$

Proof. Similar to Proposition C.2, we solve this optimization problem using the method of Lagrangian multipliers. Note that $\mathbf{w}^* = 0$. The Lagrangian is

$$\mathcal{L} = \mathbf{w}'^T \mathbf{w}' - \lambda(\mathbf{w}'^T A \mathbf{w}' - c). \quad (51)$$

Setting the derivative with respect of \mathbf{w}' to 0, we have

$$\frac{\partial \mathcal{L}}{\partial \mathbf{w}'} = 2\mathbf{w}' - 2\lambda A \mathbf{w}' = 0, \quad (52)$$

which gives

$$A \mathbf{w}' = \lambda \mathbf{w}', \quad (53)$$

so the solution to (50) is an eigenvector of A . Then, the constraint is $\mathbf{w}'^T A \mathbf{w}' = \lambda \|\mathbf{w}'\|^2 = c$, and the objective becomes $\min_{\mathbf{w}'} \|\mathbf{w}'\|^2 = \min_{\mathbf{w}'} \frac{c}{\lambda}$. Therefore, we want λ to be the largest eigenvalue of A . Hence the optimal \mathbf{w}' is an eigenvector of A corresponding to its largest eigenvalue, which is the same as the solution to (45). \square

For a more concrete example, consider a diagonal matrix A with positive diagonal elements. Then the level sets of \mathcal{L}_A are n -dimensional ellipsoids centered at the origin 0 , with axes in the same directions as the standard basis. The point with largest $\|\nabla \mathcal{L}_A\|^2$ on a level set is in the eigendirection of A corresponding to its largest eigenvalue, or equivalently, a point on the smallest semi-axes of the ellipsoid. Note that this point has the smallest distance to the global minimum $\mathbf{w}^* = 0$ among all points in the same level set. In addition, the gradient flow trajectory from this point always points to \mathbf{w}^* . Therefore, like the 2D ellipse function, one teleportation on the n -dimensional ellipsoid also guarantees optimal gradient norm at all points on the trajectory.

C.4 Relation to second-order optimization methods

To prove Proposition 5.7, we first note that when the norm of the gradient is at a critical point on the level set of the loss function, the gradient is an eigenvector of the Hessian.

Lemma C.4. *If $\partial_{\mathbf{v}} \left\| \frac{\partial \mathcal{L}}{\partial \mathbf{w}} \right\|_2^2 = 0$ for all unit vector \mathbf{v} that is orthogonal to $\frac{\partial \mathcal{L}}{\partial \mathbf{w}}$, then $\frac{\partial \mathcal{L}}{\partial \mathbf{w}}$ is an eigenvector of the Hessian of \mathcal{L} .*

Proof. From the definition of the directional derivative,

$$\partial_{\mathbf{v}} \left\| \frac{\partial \mathcal{L}}{\partial \mathbf{w}} \right\|_2^2 = \mathbf{v} \cdot \frac{\partial}{\partial \mathbf{w}} \left\| \frac{\partial \mathcal{L}}{\partial \mathbf{w}} \right\|_2^2 \quad (54)$$

Writing the last term in indices,

$$\begin{aligned} \frac{\partial}{\partial w_i} \left\| \frac{\partial \mathcal{L}}{\partial \mathbf{w}} \right\|_2^2 &= \frac{\partial}{\partial w_i} \sum_j \left(\frac{\partial \mathcal{L}}{\partial w_j} \right)^2 \\ &= \sum_j \frac{\partial}{\partial w_i} \left(\frac{\partial \mathcal{L}}{\partial w_j} \right)^2 \\ &= \sum_j 2 \frac{\partial \mathcal{L}}{\partial w_j} \frac{\partial^2 \mathcal{L}}{\partial w_i \partial w_j} \\ &= 2 \left(H \frac{\partial \mathcal{L}}{\partial \mathbf{w}} \right)_i \end{aligned} \quad (55)$$

Removing the indices,

$$\frac{\partial}{\partial \mathbf{w}} \left\| \frac{\partial \mathcal{L}}{\partial \mathbf{w}} \right\|_2^2 = 2H \frac{\partial \mathcal{L}}{\partial \mathbf{w}} \quad (56)$$

Substitute back and we have

$$\partial_{\mathbf{v}} \left\| \frac{\partial \mathcal{L}}{\partial \mathbf{w}} \right\|_2^2 = \mathbf{v} \cdot \left(2H \frac{\partial \mathcal{L}}{\partial \mathbf{w}} \right) \quad (57)$$

Since $\partial_{\mathbf{v}} \left\| \frac{\partial \mathcal{L}}{\partial \mathbf{w}} \right\|_2^2 = 0$ for all vector \mathbf{v} that is orthogonal to $\frac{\partial \mathcal{L}}{\partial \mathbf{w}}$, $\mathbf{v} \cdot \left(2H \frac{\partial \mathcal{L}}{\partial \mathbf{w}} \right) = 0$ for all vector \mathbf{v} that is orthogonal to $\frac{\partial \mathcal{L}}{\partial \mathbf{w}}$. In other words, $2H \frac{\partial \mathcal{L}}{\partial \mathbf{w}}$ is orthogonal to all vectors that are orthogonal to $\frac{\partial \mathcal{L}}{\partial \mathbf{w}}$. Therefore, $2H \frac{\partial \mathcal{L}}{\partial \mathbf{w}}$ has the same direction of $\frac{\partial \mathcal{L}}{\partial \mathbf{w}}$, and $\frac{\partial \mathcal{L}}{\partial \mathbf{w}}$ is an eigenvector of the Hessian of \mathcal{L} . \square

Proposition 5.7 is a direct consequence of Lemma C.4.

Proposition 5.7. *Let $S_{\mathcal{L}_0} = \{\mathbf{w} : \mathcal{L}(\mathbf{w}) = \mathcal{L}_0\}$ be a level set of \mathcal{L} . If at a particular $\mathbf{w} \in S_{\mathcal{L}_0}$ we have $\|\nabla \mathcal{L}(\mathbf{w})\|_2 \geq \|\nabla \mathcal{L}(\mathbf{w}')\|_2$ for all \mathbf{w}' in a small neighborhood of \mathbf{w} in $S_{\mathcal{L}_0}$, then the gradient $\nabla \mathcal{L}(\mathbf{w})$ has the same direction as the Newton's direction $H^{-1} \nabla \mathcal{L}(\mathbf{w})$.*

Proof. From Lemma C.4, $\frac{d\mathcal{L}}{d\mathbf{w}}$ is an eigenvector of H . Therefore, it is also an eigenvector of H^{-1} . Hence $\frac{d\mathcal{L}}{d\mathbf{w}}$ has the same direction as $H^{-1} \frac{d\mathcal{L}}{d\mathbf{w}}$. \square

D Experiment details and additional results

D.1 Test functions

We compare the gradient at different loss values for gradient descent with and without teleportation. Figure 7 shows that the trajectory with teleportation has a larger $d\mathcal{L}/dt$ value than the trajectory without teleportation at the same loss values. Therefore, the rate of change in the loss is larger in the trajectory with teleportation, which makes it favorable.

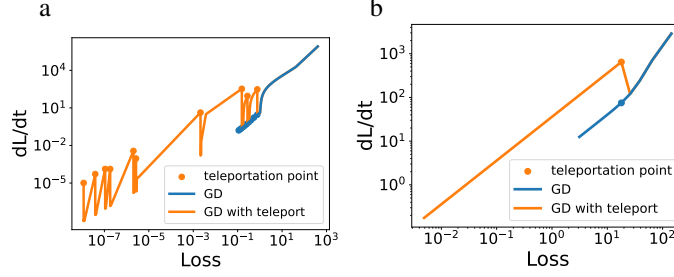


Figure 7: Gradient on the trajectory of optimizing the Rosenbrock function (left) and Booth function (right). At the same loss value, the gradient is larger on the trajectory with teleportation, indicating a better descent path.

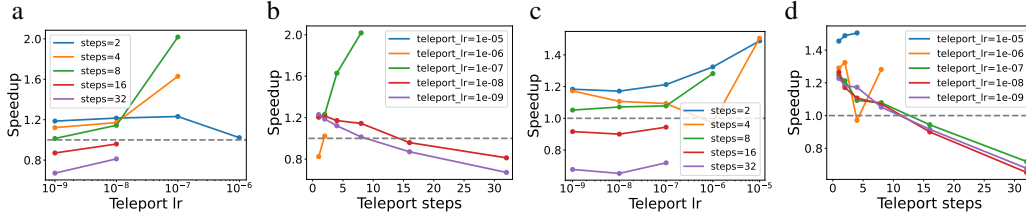


Figure 8: Hyperparameter sweeps of the number of steps and the learning rate used to find the optimal group element in teleportation. The wall-clock speedup of applying teleportation is shown separately for gradient descent (a)(b) and AdaGrad (c)(d). The dashed line represents speedup = 1.

D.2 Multilayer neural network

Additional training details Data X, Y and initialization of parameters W are set uniformly at random over $[0, 1]$. GD uses learning rate 10^{-4} and AdaGrad uses 10^{-1} . Each algorithm is run 300 steps. When using teleportation, we perform symmetry transform on the parameters once at epoch 5. In GD, the group elements used for these transforms are found by gradient ascent on T for 8 steps, with learning rate 10^{-7} . In AdaGrad, the group elements are found by gradient ascent for 2 steps, with learning rate 10^{-5} . The choice of hyperparameters comes from a grid search described in the next section.

Hyperparameter tuning To observe the effect of hyperparameters on the speedup in computation time, we did a hyperparameter sweep on the number of steps and the learning rate used in each teleportation. The speedup of teleportation on SGD and AdaGrad is defined by $t_{sgd}/t_{sgd+teleport}$ and $t_{adagrad}/t_{adagrad+teleport}$ respectively, where $t_{sgd}, t_{adagrad}$ are the wall-clock time required to reach convergence using SGD or AdaGrad, and $t_{sgd+teleport}, t_{adagrad+teleport}$ are convergence time with teleportation. We consider the optimization algorithm converged if the difference between the loss of two consecutive steps is less than 10^{-3} . This experiment is run on one CPU.

Figure 8 shows the speedup of the same multilayer neural network regression problem defined in Section 6.1, but teleporting only once at epoch 5. We did a grid search for teleportation learning rates in $[10^{-9}, 10^{-8}, 10^{-7}, 10^{-6}, 10^{-5}]$ and number of teleportation steps in $[1, 2, 4, 8, 16, 32]$. Omitted points in the figure indicate that the gradient descent fails to converge within 2000 steps or diverges.

When converged, most hyperparameter combinations improve the convergence speed in wall-clock time (speedup > 1). There are trade-offs in both the number of steps used for each teleportation and the teleportation learning rate. Increasing the number of steps used to optimize teleportation target allows us to find a better point in the parameter space but increases the cost of one teleportation. Increasing the learning rate of optimizing the group element improves $\|\partial\mathcal{L}/\partial\mathbf{w}\|$ but is more likely to lead to divergence since $\|\partial\mathcal{L}/\partial\mathbf{w}\|$ can become too large for the gradient descent learning rate.